AAAS
Ultrafast Science
Volume 2022, Article ID 9834102, 6 pages
https://doi.org/10.34133/2022/9834102

Ultrafast Science
A SCIENCE PARTNER JOURNAL

Research Article

Attosecond Delays of High-Harmonic Emissions from Hydrogen Isotopes Measured by XUV Interferometer

Mumta Hena Mustary,[1] **Liang Xu**,[2,3] **Wanyang Wu**,[2] **Nida Haram**,[1] **Dane E. Laban**,[1] **Han Xu**,[1] **Feng He**,[2,4] **R. T. Sang**,[1] **and Igor V. Litvinyuk**[1]

[1]*Centre for Quantum Dynamics, Griffith University, Brisbane, Queensland 4111, Australia*
[2]*Key Laboratory for Laser Plasmas (Ministry of Education) and School of Physics and Astronomy, Collaborative Innovation Center for IFSA (CICIFSA), Shanghai Jiao Tong University, Shanghai 200240, China*
[3]*Shanghai Key Lab of Modern Optical System, University of Shanghai for Science and Technology, 200093 Shanghai, China*
[4]*CAS Center for Excellence in Ultra-Intense Laser Science, Shanghai 201800, China*

Correspondence should be addressed to Liang Xu; liangxu2021@usst.edu.cn, R. T. Sang; r.sang@griffith.edu.au, and Igor V. Litvinyuk; i.litvinyuk@griffith.edu.au

Received 28 June 2022; Accepted 18 September 2022; Published 9 November 2022

High-harmonic spectroscopy can access structural and dynamical information on molecular systems encoded in the amplitude and phase of high-harmonic generation (HHG) signals. However, measurement of the harmonic phase is a daunting task. Here, we present a precise measurement of HHG phase difference between two isotopes of molecular hydrogen using the advanced extreme-ultraviolet (XUV) Gouy phase interferometer. The measured phase difference is about 200 mrad, corresponding to ~3 attoseconds (1 as = 10^{-18} s) time delay which is nearly independent of harmonic order. The measurements agree very well with numerical calculations of a four-dimensional time-dependent Schödinger equation. Numerical simulations also reveal the effects of molecular orientation and intramolecular two-center interference on the measured phase difference. This technique opens a new avenue for measuring the phase of harmonic emission for different atoms and molecules. Together with isomeric or isotopic comparisons, it also enables the observation of subtle effects of molecular structures and nuclear motion on electron dynamics in strong laser fields.

1. Introduction

The high-harmonic generation process is a sensitive probe of molecular dynamics and structures [1–4]. The hydrogen molecule, being the lightest, exhibits the fastest nuclear motion. Also, being the simplest neutral molecule, it allows accurate ab initio quantum mechanical simulations without resorting to severe approximations. Those simulations can be used to understand and validate the experimental results. Moreover, availability of different isotopes adds isotopic comparison as a valuable benchmarking and validation tool. A number of studies with such comparisons have already been performed, including effects of nuclear dynamics on relative HHG yields [5, 6] and tunnel ionization rates in H_2 and D_2 [7]. The strong field ionization of H_2 launches a free electron with H_2^+ in the 1 sσ_g state. The electron wave packet driven by the laser field accelerates away from the parent ion. At the same time, the nuclear wave packet evolves on the potential energy surface of H_2^+ (see Figure 1(a)). After a certain time delay, the electron wave packet returns to the parent ion upon the reversal of the driving laser field. Its consequent recombination induces an oscillating dipole, which imprints its amplitude and phase on the emitted HHG photons [8]. This ultrafast HHG process occurs in less than half of a laser oscillation period giving the potential to explore sensitive measurement on molecular electron structure and nuclear dynamics known as high-harmonic spectroscopy [9–13].

The investigation of the nuclear dynamics of hydrogen isotopes was envisioned theoretically [14–16] and implemented experimentally [5, 6, 17] by comparing their high-harmonic yields. However, only two studies explored the isotope effects on the high-harmonic phase [18, 19]. The first one estimated the relative phase by measuring harmonic yields in a mixed gas cell with H_2 and D_2 [19]. The second study relied on the determination of group delay by using the reconstruction of

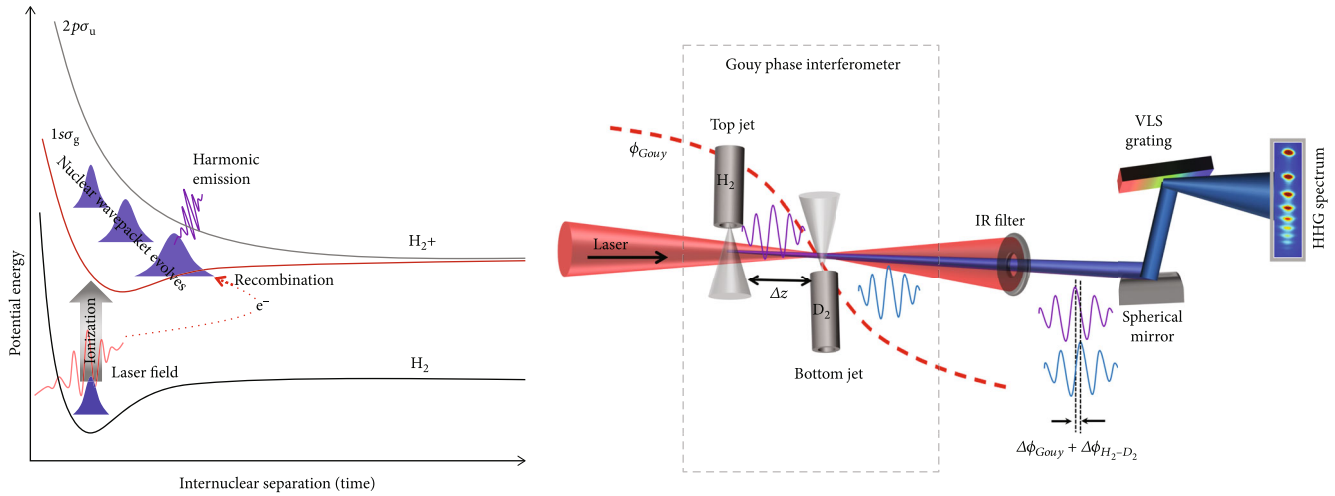

FIGURE 1: Three-step model of HHG with the potential energy surfaces of H_2 and H_2^+, and schematics of the Gouy phase interferometric technique. (a) Tunneling ionization launches an electron wave packet together with a nuclear vibrational wave packet. The ionized electron is driven by the laser electric field, and it returns to the parent ion at a certain recollision time. Simultaneously, the nuclear wave packet evolves on the potential energy surface $1s\sigma_g$ of the ground state of H_2^+. Upon electron recombination, a photon is emitted with an amplitude and phase dependent on the correlated electron-nuclear dynamics. (b) Two gas jets are placed sequentially with a separation Δz in a single laser focus. Two coherent high-harmonic pulses are generated simultaneously from the top (H_2) and bottom (D_2) gas jets. A phase difference between the two pulses includes contributions from the Gouy phase shift of the driving laser field at the two jet positions and the intrinsic phase difference between the two species. By measuring HHG yields for different gas configurations and jet separations, these two contributions can be disentangled. The XUV radiation from the first jet has negligible effect on the phase of HHG emission in the second jet as was demonstrated in [23, 24] by measuring dependence of HHG yield on separation between the jets containing the same gas.

attosecond beating by interference of two-photon transitions (RABITT) [18]. However, ensuring that both isotopes are at the same number density in the HHG interaction region is very challenging. Additionally, a sign ambiguity [19] and large experimental uncertainties of these measurements made it difficult to determine the phase difference and absolute delays accurately [18, 19]. Neither of those studies actually reproduced the measured phase difference theoretically.

To retrieve the phase information, the high-harmonic interferometers either split the driving laser beam into two paths and focus at different locations within a single gas jet that produce two phase-locked HHG photons [20, 21] or use a single driving laser beam in a gas mixture [2, 19]. The first method is limited to a single gas species, while the second has low resolution and issues with determining the sign of the relative harmonic phase. Recently, the phase difference between two atomic species was measured by an all-optical attosecond interferometric technique [22], where the delay between two extreme ultraviolet (XUV) pulses is controlled by a two-segment mirror which can provide the temporal resolution of ~6 attoseconds. Such an interferometer must maintain subcycle stability of its path difference (displacement between the two mirror segments) for XUV frequencies for the duration of the experiment, while this path difference is being scanned. This is an exceedingly difficult task which severely limits practical utility of the device.

Building an interferometer in the XUV region is quite challenging for two reasons: firstly, it is challenging to control the delay of the XUV pulses precisely between the two arms with subcycle precision; secondly, the highly reflective XUV optics is yet to be developed. Our passively stabilized Gouy phase interferometer [23, 24], on the other hand, is an all-optical direct XUV interferometric technique. It does not require calibration of gas pressures to ensure the same number densities. Additionally, it does not require any XUV optics. The technique provides an elegant way to generate two coherent high-harmonic pulses without splitting the driving laser and XUV beams. The two mutually coherent XUV pulses are generated by exploiting the inherent properties (Gouy phase) of a single Gaussian focused laser beam. This method has an unprecedented resolution of ~300 μrad (~100 zeptoseconds) because unlike other interferometric techniques, it requires optical path length stability on the order of Rayleigh length of the driving infrared laser rather than the XUV wavelength.

We apply the technique to investigate the effect of nuclear dynamics on the electron motion in molecular hydrogen by precise measurement of high-harmonic phase difference (and corresponding HHG phase delays) produced in H_2 and D_2. Since the ionization potentials of H_2 ($I_p = 15.43$ eV) and D_2 ($I_p = 15.46$ eV) are almost identical [5], the difference in the phase accumulated by electron in the continuum is considered to be negligible. However, due to the nuclear mass difference, the evolution of nuclear wave packet while electron propagates in the continuum and then recombines to the ground state may differ substantially. The harmonic intensity from the heavy isotope was shown to be

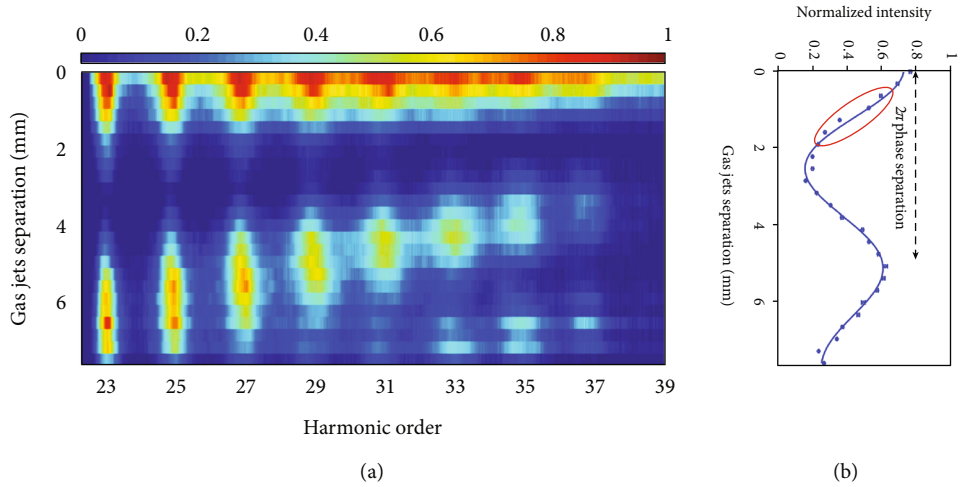

Figure 2: Normalized HHG yield from H_2 gas in both jets as a function of the jet separation. (a) Normalized HHG yield from H23 to H37. The two XUV pulses generated by a single laser pulse interfere constructively or destructively depending on the distance between the gas jets. This phase shift originates from the Gouy phase, and it follows the relationship $\Delta\phi = q\Delta\phi_{\text{Gouy}} = -q\tan^{-1}(\Delta z/z_R)$, where Δz is the separation between the jets and z_R is the Rayleigh length of the driving laser beam. (b) The normalized yield of H27 as a function of the gas jet separation. The area highlighted by the red ellipse represents the region of the highest resolution of the interferometer, i.e., where the largest HHG intensity variation occurs for a given phase shift.

higher compared to the lighter molecule as harmonic emission is sensitive to the nuclear motion [5] though for D_2, the ionization probability is less than for H_2 [7]. The aim of this work is to measure a small phase difference of HHG signals and to gain an insight into the correlated electron—nuclear dynamics for the two isotopes of molecular hydrogen.

2. Experimental Methods

The high harmonics are generated by a linearly polarized, 800 nm, 9 fs pulses with a peak intensity of $\sim 5\times10^{14}$ W/cm^2. To extract the relative phase difference between two different gases, our advanced Gouy phase interferometer consists of two spatially separated gas jets along the propagation direction in a single laser focus. One of the gas jets (bottom) is fixed in position at the center of laser focus, while the second jet (top) can move along the laser propagation direction before the focus of the laser beam, as shown in Figure 1(b) (see Supplementary Materials for details).

The Gouy phase modulates the carrier envelope phase (CEP) of a focused laser pulse which results in a phase shift of XUV pulses generated from the two gas jets given by

$$\Delta\phi = q\Delta\phi_{\text{Gouy}} = -q\tan^{-1}\left(\frac{\Delta z}{z_R}\right), \quad (1)$$

where q is the harmonic order and $\Delta\phi_{\text{Gouy}}$ is the Gouy phase difference at two gas jet positions (separated by Δz). The diameter of the gas jets is 200 μm, and gas pressure in both jets is kept at 100 Torr even though optimal phase matching happens at a slightly higher pressure. The short interaction region and low gas density help to reduce the macroscopic phase matching effects and to minimize the reabsorption of XUV photons by the second gas jet. The gases are supplied from cylinders through individual gas lines. The pressures in each gas jets are controlled by two separate regulated valves and monitored with individual capacitance manometer pressure gauges. The pressures were kept constant throughout the experiments. The gases are switched in the jets by electronically actuated microvalves that allows faster measurement and thus minimizes the errors due to laser fluctuation over time and also compensates for a small difference of intensities (and associated phases) at the two jet positions.

The interference fringes of the high harmonics from H23 to H37 generated with H_2 in both jets obtained by varying the separation between the jets are shown in Figure 2(a). To optimize the resolution for all the observable harmonic orders, the isotopic phase difference measurements were performed at jet separations of 0.63 mm and 1.27 mm where the fluctuation of laser intensities is only 0.2% and 0.8%, respectively.

To extract the relative phase difference between the harmonics generated from the two gases, for each of the two jet separations, measurements are performed for two configurations. In the first configuration, D_2 and H_2 are delivered from the top and bottom jets, respectively. The gases are swapped in the second configuration.

The HHG spectra are recorded for two different jet separations and for two gas configurations to account for systematic uncertainties. For each configuration, three HHG spectra are recorded: for both gas jets activated and for individual jet activated. The measured spectra are presented in Figure 3. The relative phase difference between H_2 and D_2 is calculated as (see Supplementary Materials for details)

$$\Delta\phi_{H_2-D_2} = \sin^{-1}\left[\frac{I_{H_2}+I_{D_2}+2\sqrt{I_{H_2}I_{D_2}}}{4\sqrt{I_{H_2}I_{D_2}}}\left(\frac{\Delta I_N}{\sin\left(q\Delta\phi_{\text{Gouy}}\right)}\right)\right], \quad (2)$$

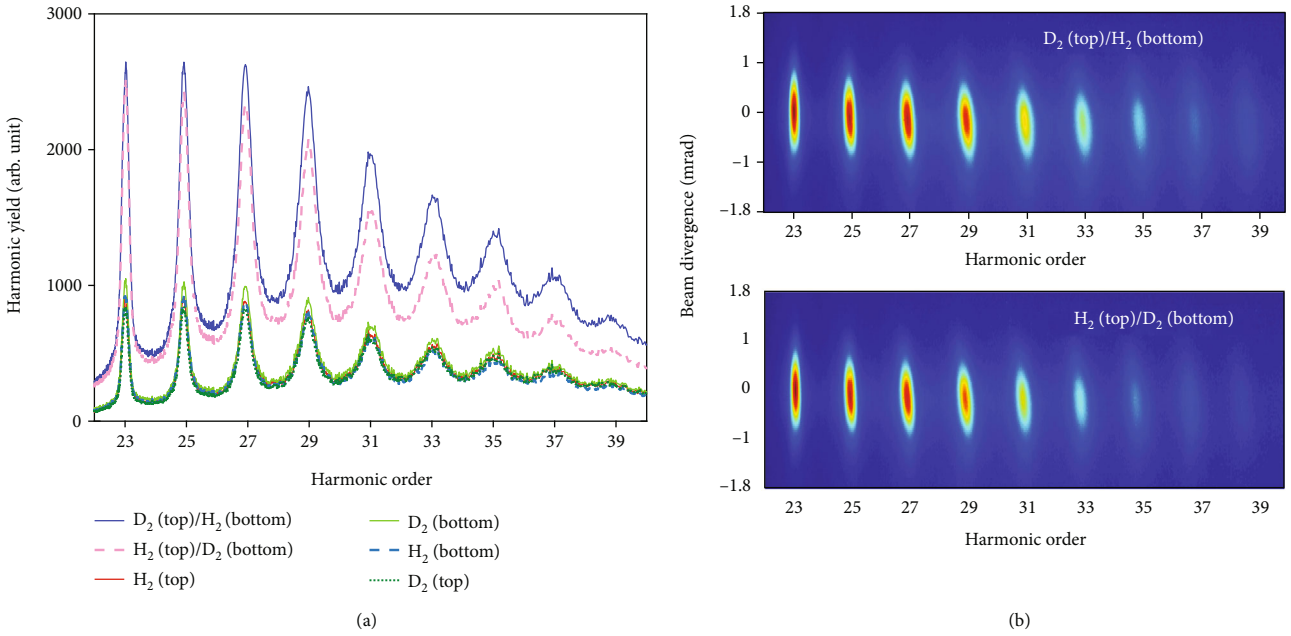

FIGURE 3: HHG spectra measured to determine the intrinsic relative phase difference between H_2 and D_2 at 0.63 mm separation between the gas jets. (a) HHG spectra for the six different gas configurations. Each spectrum is an average of 200 images. (b) Images of the top two spectra in (a) illustrating the change due to switching the order of the gases. Each image is an integrated image of 100 laser shots.

where I_{H_2} and I_{D_2} are the harmonic intensities from individual gas jets of H_2 and D_2, respectively, and $\Delta I_N = N_{D_2H_2} - N_{H_2D_2}$ is the difference in the normalized intensity obtained from the two gas configurations. Here, $N_{D_2H_2}$ is the normalized intensity when D_2 in top jet and H_2 in bottom jet, and $N_{H_2D_2}$ is normalized intensity for the opposite gas configuration.

3. Results and Discussions with Theoretical Analysis

The results are presented in Figure 4(a). The left axis corresponds to the phase difference averaged over both separations and both gas configurations. The phase differences measured at gas jet separations of 0.63 mm and 1.27 mm are very similar. This indicates that mixing of gases from the two jets has a negligible effect on our measurements. It should be noted that our method measures both the value and sign of the phase difference, and the two different configurations of gases induce opposite signs. Their absolute values were averaged, and the shown phases correspond to emission from H_2 being delayed relative to D_2 as our measurements indicate (see Supplementary Materials for details). The corresponding phase delays of harmonics from H_2 relative to D_2 are depicted on the right axis of Figure 4(a) and are determined by

$$\Delta t_{H_2-D_2} = \frac{\Delta\phi_{H_2-D_2}}{\omega_q}, \tag{3}$$

where ω_q is the angular frequency of the q^{th} harmonic order. The harmonics from H_2 are found to be ~3 attoseconds delayed in phase with respect to D_2 for all the observable harmonic orders.

The experimental measurements are supported by numerical solutions of the four-dimensional time-dependent Schrödinger equation (4D-TDSE) within the single active electron (SAE) approximation [14] (see Supplementary Materials for details). In this model, the electronic and nuclear motions are both confined to a plane containing the molecular vibration and rotation. The simulated results (red crosses) are presented in Figure 4(a), and they agree well with the experimental data (blue stars). Additional simulations showed that $\Delta\phi_{H_2-D_2}$ is relatively insensitive to the laser intensity, so the laser focal-volume averaging was not included.

According to the well-known three-step model, the total HHG phase includes contributions from the ionization, propagation, and recombination processes. Thus, for molecules aligned along different angles θ_r towards the laser polarization direction, the dynamics of ionization and recombination should be different, resulting in the θ_r-dependent $\Delta\phi_{H_2-D_2}$.

Numerically, by excluding molecular rotations and restricting the nuclear motion to vibrational degree of freedom, we reduced our 4D-TDSE model to a three-dimensional one. We used that 3D-TDSE model to obtain θ_r-dependent $\Delta\phi_{H_2-D_2}$, presented in Figure 4(b). Only the molecules aligned at small angles (0-30 degrees) from the laser polarisation direction exhibit significant dependence of $\Delta\phi_{H_2-D_2}$ on harmonic order (energy of recolliding electrons) which could be attributed to two-center interference in the recombination step. Due to the different nuclear masses, the molecular bond elongation between the ionization and recombination steps is different for H_2 and D_2. In the recombination step, the complex two-center destructive interference occurs at a specific internuclear

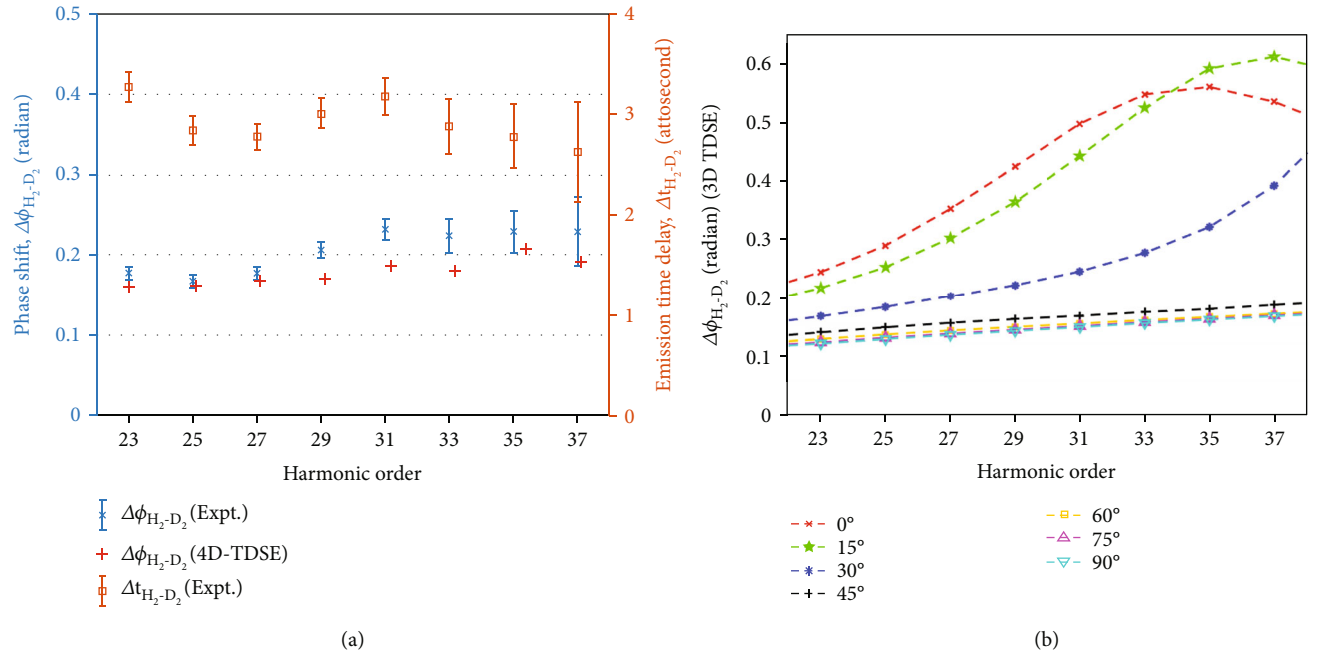

FIGURE 4: The measured relative phase difference between H_2 and D_2 isotopes from H23 to H37 and a comparison with the theoretical results analysed by TDSE numerical simulations. (a) The relative phase differences (left vertical axis, blue) and phase delays (right vertical axes, red). The red crosses represent theoretical results calculated by numerical 4D-TDSE model. (b) The phase differences between H_2 and D_2 calculated by rotation-free 3D-TDSE model for molecules aligned at different angles θ_r with respect to the laser polarization.

distance R when the recombining electron momentum k meets the condition $kR\cos(\theta_r) = \pi$, and the HHG phase undergoes a sudden change at the corresponding frequency $\omega = k^2/2 + I_p$. It is the difference in two-center interference between H_2 and D_2 that is responsible for the angle and energy dependence of the curves in Figure 4(b). More simulations show that the molecular rotation induced by the laser field results in a phase difference not more than 0.03 radian. A more detailed analysis based on the Lewenstein model and the two-center interference as well as the rotation effect estimation can be found in the supplementary information.

4. Conclusions

In summary, we have demonstrated a novel all-optical Gouy phase interferometric technique for measuring HHG phase difference between two atomic or molecular species. We used this technique to measure the HHG phase difference between H_2 and D_2 to be about 0.2 radian, corresponding to 3 attoseconds phase delay for all the harmonics. We also simulated this phase difference by numerically solving the time-dependent Schrödinger equation. The theoretical results obtained at the highest level of simulations agree quite well with the experiment. The simulations reveal that $\Delta\phi_{H_2-D_2}$ depends on the molecular alignment, the bond stretching, and the two-center interference. The phase difference of harmonics from molecular isotopes can be used as a sensitive probe of ultrafast correlated electron-nuclear dynamics in molecules.

Data Availability

The data that support the findings of this study are available from the corresponding authors upon reasonable request.

Conflicts of Interest

The authors declare that there is no conflict of interest regarding the publication of this article.

Authors' Contributions

D. L., I. L., and R. S. conceived, planned, and lead the project. M. M and D. L. set up the interferometer and the experiments. M. M. carried out the measurement, analyzed and interpreted experimental data, and improved the analysis and interpretation in discussion with D. L., I. L, and R. S. M. M wrote up experimental parts of this manuscript. L. X., F. H., and W. W. conducted numerical simulations. L. X and F. H wrote up the theoretical sections. N. H and H. X. contributed to important discussion on results and theoretical analysis. All authors contributed in discussions on the results and prepared the manuscript for submission.

Acknowledgments

The experimental research was supported by the Australian Research Council (LP140100813 and DP190101145) and Griffith University. M. M. was supported by a Griffith University International Postgraduate Research Scholarship (GUIPRS) and a Griffith University Postgraduate Research Scholarship

(GUPRS). Theoretical work was supported by the National Key R&D Program of China (Nos. 2018YFA0404802 and 2018YFA0306303), Innovation Program of Shanghai Municipal Education Commission (2017-01-07-00-02-E00034), National Natural Science Foundation of China (NSFC) (Grant Nos. 11574205, 91850203, and 12204308), and Shanghai Science and Technology Commission (Grants No. 22ZR1444100).

Supplementary Materials

Experimental setup, derivation to extract relative HHG phase shift, data analysis, TDSE simulations, the calculation parameters, further analysis based on the Lewenstein model, and estimating molecular rotation effect. Figure S1: schematic of the experimental setup. Figure S2: the calculated HHG spectra for H_2 (black line) and D_2 (red line) from 4D-TDSE simulation. Figure S3: theoretical analysis for relative phase difference between H_2 and D_2 calculated by 3D-TDSE. Figure S4: the HHG phase differences between H_2 and D_2. References [14, 24–28]. *(Supplementary Materials)*

References

[1] O. Smirnova, Y. Mairesse, S. Patchkovskii et al., "High harmonic interferometry of multi-electron dynamics in molecules," *Nature*, vol. 460, no. 7258, pp. 972–977, 2009.

[2] B. K. McFarland, J. P. Farrell, P. H. Bucksbaum, and M. Gühr, "High-order harmonic phase in molecular nitrogen," *Physical Review A*, vol. 80, no. 3, article 033412, 2009.

[3] P. Peng, C. Marceau, and D. M. Villeneuve, "Attosecond imaging of molecules using high harmonic spectroscopy," *Nature Reviews Physics*, vol. 1, no. 2, pp. 144–155, 2019.

[4] S. Biswas, B. Förg, L. Ortmann et al., "Probing molecular environment through photoemission delays," *Nature Physics*, vol. 16, no. 7, pp. 778–783, 2020.

[5] S. Baker, J. S. Robinson, C. A. Haworth et al., "Probing proton dynamics in molecules on an attosecond time scale," *Science*, vol. 312, no. 5772, pp. 424–427, 2006.

[6] S. Baker, J. S. Robinson, M. Lein et al., "Dynamic two-center interference in high-order harmonic generation from molecules with attosecond nuclear motion," *Physical Review Letters*, vol. 101, no. 5, article 053901, 2008.

[7] X. Wang, H. Xu, A. Atia-Tul-Noor et al., "Isotope effect in tunneling ionization of neutral hydrogen molecules," *Physical Review Letters*, vol. 117, no. 8, article 083003, 2016.

[8] P. Corkum and F. Krausz, "Attosecond science," *Nature Physics*, vol. 3, no. 6, pp. 381–387, 2007.

[9] T. Kanai, S. Minemoto, and H. Sakai, "Quantum interference during high-order harmonic generation from aligned molecules," *Nature*, vol. 435, no. 7041, pp. 470–474, 2005.

[10] W. Li, X. Zhou, R. Lock et al., "Time-resolved dynamics in N2O4 probed using high harmonic generation," *Science*, vol. 322, no. 5905, pp. 1207–1211, 2008.

[11] A. Zaïr, T. Siegel, S. Sukiasyan et al., "Molecular internal dynamics studied by quantum path interferences in high order harmonic generation," *Chemical Physics*, vol. 414, pp. 184–191, 2013.

[12] J. Itatani, J. Levesque, D. Zeidler et al., "Tomographic imaging of molecular orbitals," *Nature*, vol. 432, no. 7019, pp. 867–871, 2004.

[13] J. Li, J. Lu, A. Chew et al., "Attosecond science based on high harmonic generation from gases and solids," *Nature Communications*, vol. 11, no. 1, p. 1, 2020.

[14] M. Lein, "Attosecond probing of vibrational dynamics with high-harmonic generation," *Physical Review Letters*, vol. 94, no. 5, article 053004, 2005.

[15] X.-B. Bian and A. D. Bandrauk, "Probing nuclear motion by frequency modulation of molecular high-order harmonic generation," *Physical Review Letters*, vol. 113, no. 19, article 193901, 2014.

[16] L. He, Q. Zhang, P. Lan et al., "Monitoring ultrafast vibrational dynamics of isotopic molecules with frequency modulation of high-order harmonics," *Nature Communications*, vol. 9, no. 1, p. 1, 2018.

[17] P. Lan, M. Ruhmann, L. He et al., "Attosecond probing of nuclear dynamics with trajectory-resolved high-harmonic spectroscopy," *Physical Review Letters*, vol. 119, no. 3, article 033201, 2017.

[18] S. Haessler, W. Boutu, M. Stankiewicz et al., "Attosecond chirp-encoded dynamics of light nuclei," *Journal of Physics B: Atomic, Molecular and Optical Physics*, vol. 42, no. 13, article 134002, 2009.

[19] T. Kanai, E. J. Takahashi, Y. Nabekawa, and K. Midorikawa, "Observing the attosecond dynamics of nuclear wavepackets in molecules by using high harmonic generation in mixed gases," *New Journal of Physics*, vol. 10, no. 2, article 025036, 2008.

[20] M. Bellini, C. Lyngå, A. Tozzi et al., "Temporal coherence of ultrashort high-order harmonic pulses," *Physical Review Letters*, vol. 81, no. 2, pp. 297–300, 1998.

[21] C. Lyngå, M. B. Gaarde, C. Delfin et al., "Temporal coherence of high-order harmonics," *Physical Review A*, vol. 60, no. 6, pp. 4823–4830, 1999.

[22] D. Azoury, O. Kneller, S. Rozen et al., "Electronic wavefunctions probed by all-optical attosecond interferometry," *Nature Photonics*, vol. 13, no. 1, pp. 54–59, 2019.

[23] D. E. Laban, A. J. Palmer, W. C. Wallace et al., "Extreme ultraviolet interferometer using high-order harmonic generation from successive sources," *Physical Review Letters*, vol. 109, no. 26, article 263902, 2012.

[24] M. H. Mustary, D. E. Laban, J. B. O. Wood et al., "Advanced Gouy phase high harmonics interferometer," *Journal of Physics B: Atomic, Molecular and Optical Physics*, vol. 51, no. 9, article 094006, 2018.

[25] F. He, C. Ruiz, and A. Becker, "Absorbing boundaries in numerical solutions of the time-dependent Schrödinger equation on a grid using exterior complex scaling," *Physical Review A*, vol. 75, no. 5, article 053407, 2007.

[26] R. Kosloff and H. Tal-Ezer, "A direct relaxation method for calculating eigenfunctions and eigenvalues of the Schrodinger equation on a grid," *Chemical Physics Letters*, vol. 127, no. 3, pp. 223–230, 1986.

[27] J. Crank and P. Nicolson, "A practical method for numerical evaluation of solutions of partial differential equations of the heat-conduction type," *Mathematical Proceedings of the Cambridge Philosophical Society*, vol. 43, no. 1, pp. 50–67, 1947.

[28] M. Lein, N. Hay, R. Velotta, J. P. Marangos, and P. L. Knight, "Role of the intramolecular phase in high-harmonic generation," *Physical Review Letters*, vol. 88, no. 18, article 183903, 2002.